[32]J. T. Park and G. W. York, Bull. Am. Phys. Soc. 15, 1503 (1970).
[33]J. D. Bridges and W. L. Wiese, Phys. Rev. A 2, 285 (1070).
[34]D. R. Schoonover and J. T. Park, in *Proceedings of the Seventh International Conference on the Physics of Electronic and Atomic Collisions, Amsterdam* (North-Holland, Amsterdam, 1971), p. 839.
[35]J. van den Bos, G. J. Winter, and F. J. de Heer, Physica 44, 143 (1969).

PHYSICAL REVIEW A VOLUME 6, NUMBER 4 OCTOBER 1972

Ionization Cross Sections of Gaseous Atoms and Molecules for High-Energy Electrons and Positrons*

Foster F. Rieke† and William Prepejchal
Argonne National Laboratory, Argonne, Illinois 60439
(Received 31 May 1972)

Ionization cross sections of forty gases have been measured for electrons of kinetic energies 0.1–2.7 MeV. The measurements are absolute and extensive precautions have been taken to minimize systematic and accidental errors. The energy dependence of the measured cross sections is accurately described by the Bethe asymptotic formula involving two parameters that represent important atomic properties. Comparisons have been made between H_2 and D_2 and between CH_4 and CD_4; the observed differences are of the order of 1% and too small to be resolved with certainty. A close comparison has been made between positrons and electrons in Ar at 0.67 and 1.1 MeV; the cross sections are observed to be equal within a probable error of 0.5%.

I. INTRODUCTION

Although primary ionization cross sections[1] for high-energy (MeV) electrons are of practical importance and have a behavior that theoretically is simple and well understood, very few absolute values have been available from either experiment or theory. The earliest measurements[2,3] consisted in counting primary ionization events along cloud-chamber tracks. The method we have employed is based on the determination of the efficiency of a gas-filled counter in responding to monoenergetic β rays. That method was first used by Graf[4] in measurements of air and later by McClure,[5] who made measurements of H_2, He, Ne, and Ar over the energy range 0.2–1.6 MeV. Elaborating upon McClure's experiments, we have constructed an improved apparatus and studied a larger variety of gases over a somewhat wider range of energies. Throughout, we have endeavored to minimize systematic errors. The present paper is a comprehensive summary of our work, which has been described in part in the form of preliminary reports.[6–9]

To systematize the results, the Bethe theory[10–13] is employed. McClure found (and we have confirmed) that for each gas the measured cross sections are described accurately by the following relation, which he extracted from the Bethe theory,

$$\sigma = Ax_1 + Bx_2, \tag{1}$$

where

$$x_1 = \beta^{-2}\ln[\beta^2/(1-\beta^2)] - 1, \quad x_2 = \beta^{-2},$$

β = (velocity or primary electron)/(velocity of light), and A and B are empirical constants characteristic of gas.

Bethe carried out the theory in detail, with a quantum-mechanical evaluation of the constants, for hydrogenic systems only.[10] The theoretical definition of McClure's constants A and B for the general case was given by Fano.[13] Explicit formulas and a discussion of the approximations that they involve are given also in Ref. 12. As explained in Sec. 4.1 of that reference, the cross section σ_n for a fast electron to excite a target atom (or molecule) from the ground state to a state n is given by

$$\sigma_n = 4\pi(\hbar/mc)^2 (M_n^2 x_1 + C_n x_2), \tag{2}$$

where $4\pi(\hbar/mc)^2 = 1.874\times10^{-20}$ cm^2 and M_n^2 and C_n are expressed in terms of the generalized oscillator strength for the transition involved. By summation over the appropriate transitions (integration for states in the continuum), Eq. (1) is obtained in the form

$$\sigma = 4\pi(\hbar/mc)^2 (M^2 x_1 + C x_2), \tag{3}$$

which we shall use in reporting our results.

The quantity M^2 may be called the total dipole-matrix element squared for ionization, measured in units of $a_0^2 = (\hbar^2/me^2)^2$, the Bohr radius squared. In general, the M^2 for each atom or molecule includes contributions from different electron shells that are roughly proportional to the square of shell radii. Major contributions thus should stem from

outermost valence shells, and minor contributions from inner shells. Notice that most of the systems we have studied possess inner electrons only in the form of K electrons, which contribute little to the M^2.

In applying our results or in comparing them with values obtained in other types of experiment or from theory, some qualifications should be kept in mind. A total cross section σ for ionization may be considered to be a weighted sum of cross sections σ_n for excitation from the ground state to state n:

$$\sigma = \sum_n \sigma_n \eta_n \ , \tag{4}$$

where integration over the continuum is implied. In the ideal case of isolated atoms, one may usually assume that the total cross section for primary ionization is defined by the condition that the weight η_n is unity for all states above the ionization limit and zero for all states below. What we report are counting cross sections, which correspond closely, but not exactly, to the definition of primary ionization.[1] In the case of molecules, η_n may be less than unity for some states above the first ionization threshold because of the presence of rapid processes leading to neutral products, e.g., dissociation.[14] At nonvanishing pressure, η_n can be nonzero for states below the ionization limit in consequence of the following types of processes: (a) collisions of the second kind (Penning ionization),

$$A^* + B \rightarrow A + B^+ + e^- \ ,$$

which may occur in mixtures when the excitation energy of A^* exceeds the ionization energy of B; (b) associative ionization,

$$A^* + B \rightarrow AB^+ + e^- \ ,$$

which may occur when the excitation energy of A^* plus the binding energy of AB^+ exceeds the ionization energy of AB. The entities A and B may or may not be identical, so (b) may occur in pure gases as well as in mixtures.

For these reactions to influence our results, they must proceed so rapidly that ionization follows passage of the primary electron within a few microseconds, for otherwise a coincidence will not be registered. Thus, neither (a) nor (b) is likely to be of consequence if B is a trace impurity, but both must be considered in the case of gross mixtures. For example, when the pressure of B is 30 torr, a specific rate constant for (a) or (b) of 10^{-12} cm^3/sec gives a decay rate of 10^6 sec^{-1} for A^*, and the specific rate constant must be as large as 10^{-9} cm^3/sec to give the same decay rate when the pressure of B is only 0.03 torr.

II. METHOD

The method of measurement is based upon the following considerations. Primary electrons traverse a path of length L in a gas at concentration ρ; if the cross section for primary ionization is σ, the average number z of primary ionizations per electron is given by

$$z = \rho L \sigma \ , \tag{5}$$

and the probability θ that the transit of an electron produces *no* ionization is given by

$$\theta = e^{-z} \ . \tag{6}$$

Thus, by measuring θ, with ρ and L known, one can determine σ.

The apparatus is illustrated schematically in Fig. 1. Electrons from a β emitter J are selected for energy by the magnetic analyzer M, pass through the thin-window gas-filled counter G, and fall upon the silicon barrier-layer detector D. A pulse in channel $d \cdot g$ indicates that a primary electron has passed through G and resulted in ionization; a pulse in channel $d \cdot \bar{g}_s$ indicates that a primary has passed through without producing any ionization. The "stretch" is introduced in order to exclude from channel $d \cdot \bar{g}_s$ pulses from D that occur within the dead time during which G is allowed to recover its full sensitivity after having responded to ionization. If in an observation period u counts accumulate from channel $d \cdot g$ and w counts from $d \cdot \bar{g}_s$, the probability ϕ that the transit of a primary through G does not give rise to a count from G is given by

$$\phi = w/(u + w) \tag{7}$$

with a relative standard deviation $\delta\phi/\phi$ given by

$$(\delta\phi/\phi)^2 = (1 - \phi)/w. \tag{8}$$

Were it not for wall effects in G, ϕ could be iden-

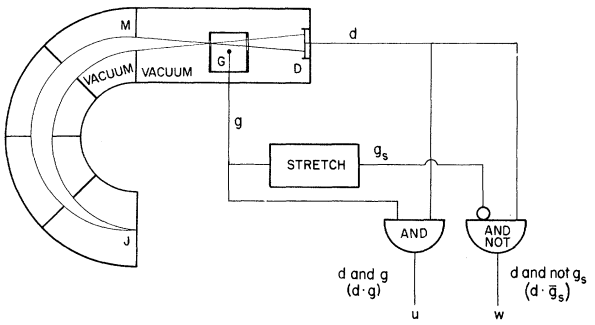

FIG. 1. Schematic diagram of the apparatus. The double-focusing magnetic analyzer M selects electrons (or positrons) of a definite momentum in the β rays from the source J. An electron hitting the silicon detector D causes a pulse in channel d. An ionization event in the gas counter G causes a pulse in channel g, and after the "stretch", a pulse in channel g_s. The number of counts in channel $d \cdot g$, i.e., "d and g," is u, and that in channel $d \cdot \bar{g}_s$, i.e., "d and not g_s," is w.

tified with θ of Eq. (6).

Wall effects may be expected, however, both because some of the electrons liberated from the gas in close proximity to either window of G are lost by diffusion to the window, and because there is some secondary emission of electrons by the windows into the gas. The probability that all of the electrons liberated in a primary ionization that occurs at a distance x from a window diffuse to the window must be a function of (ρx); when this probability is averaged over x the result is inversely proportional to ρ. Thus the effective number of primary ionizations per primary electron is the z of Eq. (5) multiplied by $(1-\lambda/\rho)$, where λ is an undetermined constant characteristic of the gas. Secondary emission by the windows will, for each primary, on the average give rise to z_s electrons that reach the sensitive volume of G. When both the above effects are taken into account, the probability that the transit of a primary electron leads to *no* response from G is $\exp[-\rho L\sigma(1-\lambda/\rho)-z_s]$, which may be equated to the ϕ of Eq. (7) to obtain the relation

$$y \equiv -\ln[w/(u+w)] = LN_L\sigma p + y_0, \tag{9}$$

where N_L is Loschmidt's number, p is the gas pressure reduced to 0 °C, and $y_0 = -L\lambda\sigma + z_s$, a function of primary energy.

By measuring y at a series of pressures, σ can be derived from the best straight-line fit of y plotted against p. In turn, to make connection with Eq. (3), values of σ/x_2 obtained for a series of primary energies may be plotted against x_1/x_2, as suggested by Fano[13]; the points should fall on a straight line with slope M^2 and intercept C, apart from the universal constant $4\pi(\hbar/mc)^2$. This procedure was carried out for several gases; the results showed that the energy dependence of the cross sections followed Eq. (3) within experimental error. We then abandoned the successive curve fittings in favor of a single least-squares solution to determine M^2 and C directly from the entire collection of experimental points $[y, p, x_1(\beta), x_2(\beta)]$ obtained for each gas. To make a least-squares solution feasible, y_0 (a smooth function of primary energy) is represented as a linear combination of x_1 and x_2; Eqs. (3) and (9) are then combined into

$$y/[4\pi(\hbar/mc)^2 LN_L] = M^2 x_1 p + C x_2 p + c_1 x_1 + c_2 x_2. \tag{10}$$

(The quantity y_0 is sufficiently small that arbitrarily setting it equal to zero would lead to values of M^2 and C within 10% of those we obtain.)

III. EXPERIMENTAL DETAILS

Referring to Fig. 1, the source of electrons J is Pr^{144} in equilibrium with Ce^{144}, which emits a continuous spectrum of β rays with upper limit 3 MeV. The double-focusing magnetic analyzer M has a resolution of 1% in momentum; its calibration, momentum vs magnet current, is based on the Cs^{137} conversion line and is extended to higher and lower energies by means of gaussmeter readings. The gas-filled counter G is designed to fulfill the following requirements: The path of the primary electrons between entrance and exit windows should have a well-defined length; the entire path of every primary should be contained within the sensitive volume of the counter with none being intercepted by the center wire; and the potential distribution about the center wire should be symmetrical. As constructed, it has a 1.27-cm-square bore with wire centered in the bore. The windows, of 0.006-mm gold-coated Mylar, are flush with opposing walls and are so placed that the axis of the primary beam passes midway between the center wire and one wall. The walls are of brass with gold coating.

The most critical factor in the accuracy of the results is the reliability of the gas-filled counter and its associated electronics, which should register a count unfailingly whenever one or more primary ionizations occur within the gas. Inasmuch as single-electron events are the ones most likely to be missed, the problem is primarily that of detecting such events. Because the gas under investigation must serve as the counting gas, it is necessary to establish satisfactory counting conditions for each gas at each of the pressures used.

The detection of single slow electrons in a gas is accomplished through amplification by electron avalanche. The gases more or less fall into two classes. In one class a moderately large avalanche gain leads reliably to successive avalanches (avalanche breeding); such gases lend themselves to a breakdown (GM) mode of counting. In the other class, avalanche breeding occurs reluctantly and unreliably even with a very large average single-avalanche gain; these cases lend themselves to proportional counting (PC) or, more descriptively, prebreakdown counting.

Our experience with PC closely parallels that described by Gold and Bennett.[15] For single-electron events the pulse-height spectrum is very broad and obviously extends below the discriminator level that excludes amplifier noise. A correction for lost small pulses can be estimated by extrapolating the spectrum below the discriminator level, but the correction is large and uncertain unless the average avalanche gain is very large. We have employed PC only for those gases that permit a large avalanche gain and we operated the counter at voltages near the point where a continuous discharge tended to occur. (That under such conditions many pulses saturate the amplifier is of no consequence in our measurements, which

depend only upon detection and not at all upon pulse-height linearity.) In consequence, the corrections for lost small pulses usually contributed less than 5% to the total, and the values of y that resulted were insensitive to variations in counter voltage.

The following considerations apply to GM counting. The gases under investigation do not provide self-quenching action and the addition of a quenching agent would increase considerably the uncertainty in the measured cross section; therefore external quenching must be used. For single-electron events, the plateau curve rises comparatively slowly as the voltage is raised above threshold, so the counter must be operated far above threshold if such events are to be detected reliably. As the overvoltage is raised, however, the self-generated background of the counter increases. A fairly large background can be tolerated, since the coincidence arrangement discriminates strongly against random counts from the gas-filled counter, but the random counts increase the deadtime and thus slow down the accumulation of data. The rate of generation of false counts decreases with time after a discharge, and stable operation is possible only with a long quench pulse. In some cases it is necessary to hold the voltage below threshold for as long as $\frac{1}{2}$ sec in order to allow complete recovery from the preceding discharge. The quenching circuit used is described in the Appendix.

Pressures in the gas cell were measured with a Wallace & Tiernan gauge that was calibrated against a Texas Instrument Co. fused-quartz Bourdon gauge. We estimate the error in the pressure measurement to be 0.05 torr or less. Because of distortion of the thin windows, the path length depends, to a small degree, upon the gas pressure. The distortion has been measured and allowed for in the calculations by adding small corrections to the observed pressures. The path length has also been corrected to take into account scattering of the primary electrons by the entrance window. Calculations showed that at 0.1 MeV the average path of the primaries between entrance and exit windows is 1.5% greater than the distance between windows; the difference becomes negligible for energies above 0.5 MeV.

The materials studied were usually the purest available commercially. The H_2 and D_2 samples were purified by diffusion through palladium, and all liquids were degassed under vacuum in order to remove dissolved permanent gases. The He, Ne, Kr, Xe, and N_2 samples were research grade from Air Products and Chemicals, Inc., while the CH_4, C_2H_6, C_3H_8, n-butane, neopentane, C_2H_4, propene, and C_6H_6 samples were research grade from the Phillips Petroleum Company. The Matheson Company supplied the Ar and CO_2 samples (research grade), the CO, H_2S, BF_3, and i-butane samples (cp grade), and the NO, NH_3, PH_3, CF_4, $(CN)_2$, cyclopropane, C_2H_2, and $(CH_3)_2O$ samples. The Matheson, Coleman, and Bell Company supplied the cyclohexane, CH_3OH, and acetone samples (chromatoquality), as well as the n-pentane, n-hexane, and n-heptane samples (spectroquality reagent). The O_2 sample was research grade from the Air Reduction Company, the CD_4 sample was from the Volk Radiochemical Company, and the C_2H_5OH sample was reagent grade from the U. S. Industrial Chemicals Company. The mercury sample was triple distilled and distilled water was used.

The measurements on mercury vapor were made using a different counting chamber constructed of stainless steel with seals made with silicon rubber or Teflon and windows of Mylar with additional nickel windows to define the path length. The mercury vapor pressure was calculated from temperature measurements at a mercury cold-finger reservoir that was maintained at a regulated temperature. The temperature was measured with a platinum resistance thermometer and the vapor pressure of mercury was calculated using Eq. (19) given by Carlson, Gilles, and Thorn[16] to apply to data by Busey and Giauque.[17] It was especially difficult to obtain reliable counting characteristics with mercury vapor, so these results are subject to greater uncertainty than for most of the other gases.

IV. ERROR ANALYSIS

Errors may best be discussed in relation to the Bethe formula. This formula is expected to describe accurately the energy dependence of cross sections throughout and well beyond the range of our measurements; within their limits, the measurements conform to this expectation and an illustration of this is given in Sec. V. Equation (3) may be rewritten in the form

$$\sigma = (1.874\times10^{-20}\ \mathrm{cm}^2)\, C[(M^2/C)x_1 + x_2]. \qquad (11)$$

Its form is illustrated in Fig. 2, where σ/C is plotted against $\log_{10}E$ for the values of $M_2/C = 0.08$, 0.10, and 0.12. Among our results, the values of C range from 7 to 250, while M^2/C is confined to the limits 0.086–0.123. The quantity C may be regarded as the scale factor and M^2/C as the shape parameter for the curve.

Generally speaking, C represents an average over all data points, and its value is rather insensitive to errors in individual points. On the other hand, M^2/C is determined by the ratio (cross section at high energy)/(cross section at low energy). Taking cross sections at the two limits of our energy range, the ratio is 0.453 for $M^2/C = 0.092$ and 0.502 for $M^2/C = 0.123$. From these numbers

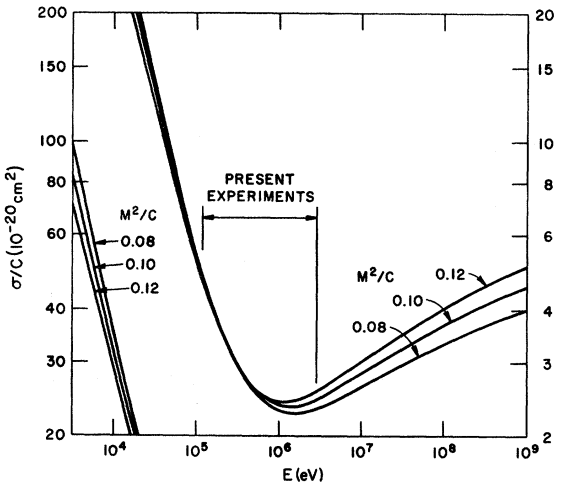

FIG. 2. Bethe formula σ/C as a function of primary kinetic energy E, with M^2/C as a parameter. The vertical scale on the left applies to lower E, and that on the right to higher E.

it is evident that M^2/C is very sensitive to errors toward either end of the energy range and can be determined only with a much lower relative precision than can C. Conversely, given an accurate value of C, cross sections can be computed quite accurately and extrapolated over a wide energy range in spite of a relatively large uncertainty in M^2/C.

For each gas studied, values of M^2 and C are derived from a collection of usually thirty or more data points. A quantitative estimate of the limits of errors is necessarily rather complicated and tedious; the method will be sketched only briefly.

For an analysis of errors it is convenient to recast Eq. (10) in the form

$$y/[4\pi(\hbar/mc)^2(LN_L)(1-\epsilon)] = C_0 p_{\min}[(M^2/C_0)x_1+(C/C_0)x_2](p/p_{\min}) + p_0(0.1x_1+x_2), \quad (12)$$

where ϵ represents the probability that the counting mechanism fails to register a valid ionization act. Further, C_0 is a "standard" C value and $p_{\min}$ is the smallest pressure value used in a run of measurements. Finally, the last term $p_0(0.1x_1 + x_2)$ approximates the $c_1x_1+c_2x_2$ in Eq. (10), p_0 being a constant with the dimension of pressure. This approximation is permissible because that term is always small and M^2/C is never very different from 0.1.

Suppose that during the measurements the actual values of β and p differ from those given by the meter readings and calibrations by $\Delta\beta$ and Δp, and that ϵ is finite though small. When the observed values are put into a least-squares solution for M^2 and C, values differing from the true ones by ΔM^2 and ΔC are obtained. We wish to find how $\Delta C/C$ and $\Delta(M^2/C)$ are related to the ϵ, $\Delta\beta/\beta$, and $\Delta p/p$.

Systematic Errors

Systematic errors are those that result from errors of calibration for L, β, and p, and from nonideal counting conditions for ϵ.

The case of L is trivial; the uncertainty in the path length is not greater than 1/2%; it contributes 0.005 to $\Delta C/C$ and virtually 0 to $\Delta(M^2/C)$.

The systematic errors in β may be different for different values of β, but do not vary from data point to data point taken at the same β. We estimate the maximum magnitude $\Delta\beta/\beta$ to be 0.01. Similarly for p, we estimate the error in calibration of the Wallace & Tiernan gauge to be not greater than 0.05 torr, and the estimated uncertainty in the pressure determination for mercury is less than 1%. Counting conditions vary from gas to gas and from pressure to pressure for the same gas. Conditions are tested for each combination of gas and pressure by observing y at successively higher counter voltages with β near the value for minimum ionization. Conditions are considered satisfactory when the variation with voltage does not exceed the statistical uncertainty in y; counting is continued until the standard deviation (absolute, not relative, deviation) in y, based on counted numbers, is 0.01. We conclude that ϵ must lie between zero and 0.02 except perhaps in a few difficult cases.

The effects of systematic errors must depend on the values of β and $p/p_{\min}$ and the actual distribution was simulated in a calculation.[6(e)]

By partial differentiation of Eq. (12), dy can be computed for any combination of $d\beta/\beta$, $d\epsilon/\epsilon$, and dp/p for the individual points. One can then relate the values of dC/C and $d(M^2/C)$ to any small variations of β, ϵ, and p. Because of the correlations of the errors, it is convenient to label the y's with indices i, j to represent momentum i, pressure j. Because ϵ is correlated with p, it also carries the index j.

The least-squares method expresses M^2 and C as linear functions of the y_{ij}:

$$C=\sum_{ij}A_{ij}y_{ij}, \quad M^2=\sum_{ij}B_{ij}y_{ij},$$

where A_{ij} and B_{ij} are independent of the y_{ij}. Thus, $A_{i'j'}$ and $B_{i'j'}$ can be evaluated by comparing two least-squares solutions that are exactly the same except for a variation in $y_{i'j'}$. The numerical work was carried out for $M_0^2/C_0=0.105$, a median value, and $LC_0p_{\min}$ so chosen to yield a typical range of y_{ij}. (The range tends to be much the same for all experiments).

From the expression

$$dC/C= C^{-1}\sum_{ij}\partial C/\partial y_{ij}[\beta_i(\partial y_{ij}/\partial\beta_i)(d\beta_i/\beta_i)$$

$$+p_j(\partial y_{ij}/\partial p_j)(dp_j/p_j) - y_{ij}\epsilon_j] \,, \quad (13)$$

one can compute the error $\Delta C/C$ that results from any combination of errors $\Delta\beta_1/\beta_1$, $\Delta\beta_2/\beta_2$, ..., $\Delta p_1/p_1$, $\Delta p_2/p_2$, ..., ϵ_1, ϵ_2 .... A relation analogous to Eq. (13) for dM^2 can be written, and from

$$d(M^2/C) = C^{-1}(dM^2 - M^2 dC/C),$$

$\Delta(M^2/C)$ can be evaluated.

The results show that the contribution to $\Delta C/C$ from errors in β, p, and ϵ is ± 0.0053, $\pm (0.0221/p_{\min})$, and $+0.0043$ or -0.0244, respectively, while the contribution to $\Delta(M^2/C)$ from these sources is ± 0.0041, $\pm (0.0058/p_{\min})$, and ± 0.0046, respectively. The limit of systematic error is then found by choosing the combination of signs that maximize the error after including the contribution from the error in L. These limits are given in Table I.

Random Errors

The term random errors is usually applied to errors that arise from truly capricious aspects of an experiment such as noise, statistical errors in counting, and chance errors in reading instruments. According to the theory of the method of least squares, the uncertainty in our values for M^2 and C should be given by multiplying the root-mean-square deviation of the individual y's by certain coefficients that come out of the least-squares solution. The uncertainty due to random errors should then be added to that due to systematic errors. Such a procedure in our case, however, is not completely valid, inasmuch as some of the errors we have treated as systematic can also contribute to the root-mean-square deviation of the data points.

Our standard practice has been to accumulate counts until y has been determined with a statistical accuracy of 0.01. Points of that or better accuracy are given unit weight in the least-squares solution; points of less accuracy are given appropriately smaller weight. In some cases, the root-mean-square deviation turns out to be very nearly 0.01; in others, as much as 2.8 times as great. The difference cannot be attributed to genuinely random effects; we attribute it to variations in ϵ, which have been treated as systematic error. We conclude that the true random error in our experiments can be estimated reasonably well by multiplying the coefficients from the least-squares solution by 0.01. It is the random error so obtained that should be added to the systematic errors indicated in Table I. The coefficients vary from experiment to experiment because they depend upon the number and distribution of the data points. For most gases, $\Delta C/C$ range from 0.002 to 0.012 and $\Delta(M^2/C)$ range from 0.0015 to 0.004.

V. RESULTS

The values of M^2 and C for the various gases studied are given in Table II. With the aid of these values and Fig. 2, the ionization cross section at any energy where the Bethe formula is applicable can be obtained by simple multiplication.

The data in Table II represent final and comprehensive results of our series of measurements, and thus supersede all the preliminary data reported in Refs. 6–9.

Figures 3 and 4 exemplify the fit of our data to the Bethe formula, Eq. (3). In these figures, the ordinate represents $x_2^{-1}\sigma/1.874\times10^{-20}$ cm$^2 = \beta^2\sigma/1.874\times10^{-20}$ cm^2 and the abscissa $x_1/x_2 = \ln[\beta^2/(1-\beta^2)] - \beta^2$. The straight line is drawn with the slope M^2 and the intercept C at $x_1/x_2 = 0$, both determined from the least-squares solutions described in Sec. IV. The data for isobutane in Fig. 3 closely follow the straight line. The data for xenon in Fig. 4 show somewhat larger scatter, but no significant trend of a departure from the straight-line behavior. (For an atom as heavy as xenon, binding energies of electrons in inner shells are appreciable compared to the incident energies of the electrons used in our experiment, so that a departure from the Bethe formula might be expected).

In some cases it was necessary to add a few torr of H_2 or CH_4 to achieve GM counting. In these cases the cross section includes contributions from excitation to excited states, caused by excited states that transfer their energy to produce Penning ionization of the additive. Also, we have found that in highly pure helium the GM discharge is much delayed, so that coincidences do not occur within the 5 μsec allowed by the coincidence circuit. Addition of a very small amount (0.01 torr) of impurity, such as hydrogen or argon, eliminates the delay. We have interpreted[6(c)] this behavior to mean that photoionization in the gas is necessary for rapid avalanche breeding, and that a very small amount of a component that can be photoionized by helium resonance radiation is effective. The small amount of argon, however, may be ionized to some extent via energy transfer from helium excited states, as discussed at the end of Sec. I.

TABLE I. Limits of systematic errors.

$p_{\min}$	$\Delta C/C$ Max.	$\Delta C/C$ Min.	$\Delta(M^2/C)$
1 torr	0.04	−0.06	±0.015
10 torr or more	0.02	−0.04	±0.009

TABLE II. Values of M^2 and C for all the gases studied.

Gas	Additive[a] Pressure (torr)	Gas	Pressure range (torr)	No. of data points	rms residual[b]	M^2 Value	M^2 s.d.[c]	C Value	C s.d.[c]	Quality estimate[d]
He[e]	0.01	Ar	19 –110	50	0.012	0.774	0.030	7.653	0.037	*A*
He[e]	4.6	H_2	14 – 86	43	0.008	0.745	0.025	8.005	0.032	*A*
He[e]	3.8	CH_4	15 – 70	47	0.011	0.738	0.032	7.056	0.040	*A*
Ne[e]	0.01	H_2	9 – 64	45	0.008	2.02	0.05	18.17	0.06	*A*$^+$
Ne[e]	3.8	H_2	10 – 51	32	0.014	2.11	0.11	18.41	0.15	*B*
Ar[e]	1.05	H_2	4.6– 38	37	0.014	3.69	0.12	38.14	0.19	*B*
Ar[e]	...[a]	...	7.4– 32	31	0.009	4.22	0.15	37.93	0.19	*A*
Kr[e]	3.8	H_2	3.7– 38	41	0.018	6.09	0.16	52.38	0.22	*A*$^-$
Xe[e]	3.8	H_2	3.6– 16	35	0.012	8.53	0.35	74.17	0.51	*B*$^-$
Xe[e]	...	...	2.4– 13.7	57	0.013	8.04	0.15	72.35	0.40	*A*
Hg[e,f]	...	...	0.3– 6.7[f]	23[f]	0.015	5.69[f]	0.94[f]	63.8[f]	2.0[f]	*C*
H_2+D_2[e]	...	...	36 –183	242	0.013	0.695	0.015	8.115	0.021	*A*
H_2+D_2[e,g]	...	...	36 –128	46	0.019	0.48	0.15	8.148	0.061	*B*$^+$
N_2[e]	3.8	H_2	7.4– 28	52	0.013	3.74	0.14	34.84	0.20	*A*$^-$
O_2[e]	...	...	5 – 23	57	0.024	4.20	0.18	38.84	0.47	*C*
CO[e]	3.8	H_2	9 – 18	44	0.011	3.70	0.15	35.14	0.19	*B*$^+$
NO[e]	...	...	4 – 18	26	0.016	4.31	0.48	42.26	0.57	*B*$^-$
H_2O[e]	...	...	4 – 12	51	0.012	3.24	0.15	32.26	0.47	*B*
H_2S[e]	...	...	2 – 11	34	0.016	5.03	0.27	42.19	0.58	*B*
CO_2[e]	...	...	7 – 21	44	0.012	5.75	0.10	55.92	0.40	*A*$^-$
CO_2[h]	...	...	7.4– 23	47	0.011	5.75	0.073	57.91	0.27	*A*
NH_3[e]	0.9	H_2	3 – 8	33	0.010	3.58	0.35	34.86	0.44	*C*
PH_3[e]	...	...	2 – 12	48	0.010	4.57	0.18	45.90	0.42	*A*
BF_3[e]	...	...	4.4– 13	39	0.012	7.04	0.48	64.29	0.54	*A–B*
CF_4[e]	...	...	1.3– 11	31	0.023	10.26	0.77	84.05	1.47	*C*
$(CN)_2$[e]	...	...	3.3– 7.4	31	0.013	7.27	1.12	72.16	1.35	*B*
CH_4+CD_4[h]	...	...	5 – 37	129	0.016	4.23	0.13	41.85	0.20	*A*$^-$
CH_4+CD_4[g,h]	...	...	5 – 28	42	0.015	3.69	0.74	43.88	0.25	*B*
C_2H_6[h]	...	...	4 – 27	35	0.018	6.80	0.36	68.93	0.55	*B*
C_3H_8[h]	...	...	3 – 14	48	0.012	11.93	0.43	114.10	0.66	*A*$^-$
n-butane[h]	1	CH_4	3 – 7	35	0.010	16.80	0.45	152.5	0.58	*A*
i-butane[h]	...	...	2.3– 9.2	45	0.012	14.19	0.20	141.9	0.63	*A*
n-pentane[h]	...	...	1.9– 8.3	45	0.014	18.41	0.33	184.8	1.00	*A*$^-$
neopentane[h]	...	...	1.1– 8.3	44	0.028	19.61	0.61	182.9	1.65	*B*$^-$
n-hexane[h]	...	...	1.9– 5.8	41	0.015	23.0	0.40	223.4	1.6	*B*
n-heptane[h]	...	...	1 – 5.5	44	0.015	25.1	0.46	256.2	1.6	*B*
cyclopropane[h]	...	...	2.9– 12.1	47	0.012	10.61	0.17	106.2	0.57	*A*
cyclohexane[h]	...	...	1.5– 9.3	55	0.017	21.97	0.36	213.2	1.13	*B*$^+$
C_2H_2[h]	...	...	9.2– 27.4	47	0.014	5.21	0.086	53.76	0.36	*A–B*
C_2H_4[h]	...	....	4.2– 18.5	39	0.011	6.75	0.10	68.82	0.33	*A*$^-$
propene[h]	1	CH_4	5 – 11	40	0.024	9.85	0.66	87.23	0.83	*C*
C_6H_6[e]	...	...	1.0– 4.4	58	0.009	17.54	0.37	162.4	1.1	*A*
CH_3OH[h]	...	...	4.7– 20	54	0.023	6.22	0.18	66.40	0.64	*B*
C_2H_5OH[h]	...	...	4.2– 12	44	0.020	9.94	0.27	97.66	0.99	*A*$^-$
acetone[h]	...	...	3.0– 9.8	48	0.015	11.89	0.24	118.0	0.80	*A*$^-$
$(CH_3)_2O$[h]	...	...	3.1– 13.7	42	0.012	10.17	0.14	105.2	0.47	*A*

[a]No entry in this column means that the pure gas was used with no additive.

[b]Root-mean-square deviation, discussed in text.

[c]Standard deviation estimated from least-squares analysis.

[d]The experimentalists' estimate of the reliability of the data with *A* being the best and *C* the worst.

[e]Data obtained using GM counting.

[f]Data for Hg are more uncertain; see text.

[g]Data obtained using positrons.

[h]Data obtained using proportional counting.

Isotope Effects

The ionization cross section of a molecule, as opposed to an atom, should change, in general, upon an isotopic substitution of its constituent nuclei. A significant isotope effect may be expected when a substantial fraction of ionizing events occur via preionization of superexcited states, as

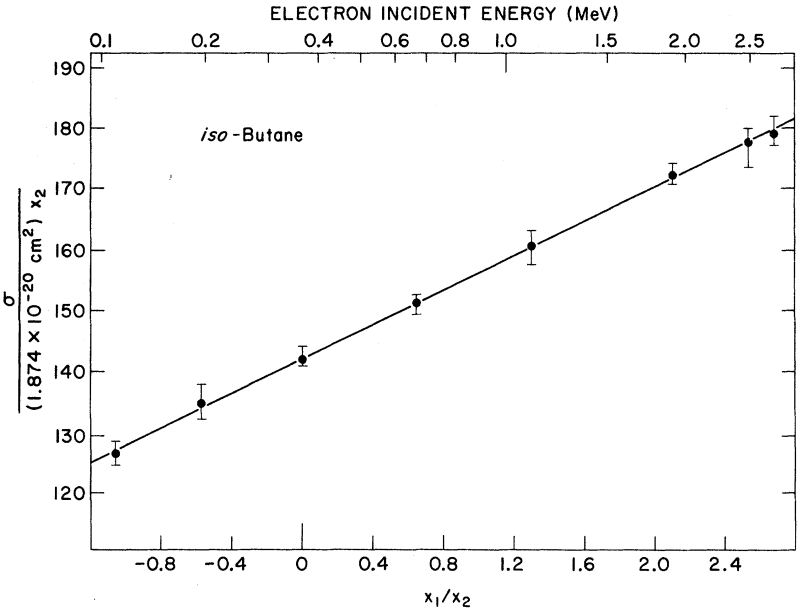

FIG. 3. Data for isobutane displayed on the Fano plot (Ref. 13). On the top, a nonlinear scale for electron energy is shown. The straight line corresponds to the result, given in Table II, of a comprehensive analysis of all data taken at pressures between 2.3 and 9.2 torr. This analysis also determined the value of p_0 that was used in Eq. (12) in order to plot the data taken at different pressures. The weighted average of the data points thus corrected is shown by a dot at each β value. The vertical bar embracing the dot represents the full range of data at different pressures.

first predicted by Platzman.[18,19]

Comparisons were made between CH_4 and CD_4 and between H_2 and D_2. In attempting to summarize the results it was observed that the differences were correlated with differences between the p_0 term in Eq. (12). These differences seem to be connected with chance failures to obtain maximum counting efficiency, particularly at high pressures, i.e., with chance occurrences of systematic errors. Consequently, the data for both isotopic molecules were used in a single least-squares solution and then the residuals were analyzed separately. For hydrogen, the average value of y is 0.86 and the average residual ($y_{obs} - y_{calc}$) for H_2 is -0.0054, and for D_2 is $+0.0055$. This represents an isotopic effect of 1.3%, so the increase in ionization in D_2 is not larger than the experimental uncertainty. For methane, the average value of y is 0.80 and the residuals average -0.0013 for CH_4 and 0.0025 for CD_4. This represents an isotope effect of 0.5%, with the possible error at least as great. The lack of a clear isotope effect is the justification for the combination of data from both isotopes in Table II.

Although the isotope effects observed are not large in comparison with the probable errors, the effects do have the direction of the Platzman prediction that heavier isotopic molecules should have greater ionization. Furthermore, our results are of the same magnitude as the isotope effects observed by Jesse[20] in his high-precision measurements of the total ionization produced when a β particle (mean energy about 18 keV) loses all its energy in a gas. Jesse found 0.6% greater ionization for CD_4 than for CH_4 and 0.8% greater ionization for D_2 than for H_2.

Comparison of Ionization by Positrons and by Electrons

According to the first Born approximation, on which the Bethe theory is based, the cross section for any inelastic collision with any atom or molecule is proportional to the square of the charge on the incident particle. Thus, the first Born ap-

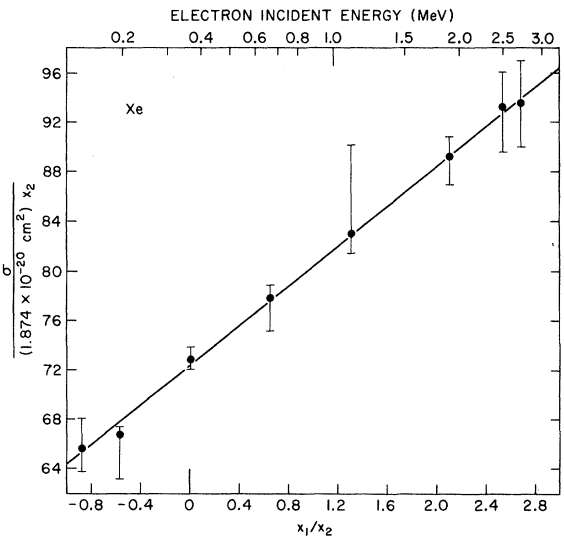

FIG. 4. The data for Xe displayed on the Fano plot (Ref. 13). On the top, a nonlinear scale for electron energy is shown. The straight line, the dots, and the vertical bars signify the same as in the caption for Fig. 3, except that the pressure range over which data were taken is between 2.4 and 13.7 torr.

proximation predicts identical cross sections for ionization by a positron e^+ and by an electron e^- at the same kinetic energy.

Included in Table II are entries corresponding to determinations of M^2 and C for e^+ as well as for e^- for the cases of hydrogen and methane. We can attach quantitative significance only to $C_{e^+} - C_{e^-}$; the uncertainty in M^2 for e^+ is large because of the small energy range. For H_2 and D_2, $(C_{e^+} - C_{e^-})/C_{e^-}$ is +0.004, a value less than the experimental uncertainty; for CH_4 and CD_4 the value is 0.048, a value larger than expected for a random error but not outside the systematic error limit. In both of those experiments it was necessary to expose the counting chamber to the atmosphere while changing the source between e^- and e^+. In order to make a more definitive test, we made a separate experiment on argon, using a source that emitted both e^+ and e^-, which allows the comparison without changing sources. (The slight differences in incident energy of the e^+ and e^- were compensated by measuring the magnetic field strength in the analyzer.) Table III gives the results measured in argon (pressure about 14 torr) at two energies; they show the ionization cross sections agreeing within the statistical uncertainty of the data.

The absence of a positron-electron difference may be considered as another indication of the applicability of the Bethe theory in addition to the fitting of our data to the energy dependence given by Eq. (3).

Data for Mercury

Mercury gave special experimental difficulties and the data in Table II may be subject to greater uncertainty than indicated by the standard-deviation estimates. In particular, the data at pressures of 1.9 to 6.7 torr indicate a value of p_0 in Eq. (12) that is inconsistent with data taken at 0.3 torr. If the 0.3-torr data are removed and the 17 data points remaining are analyzed, then one estimates $M^2 = 5.96 \pm 0.85$ and $C = 59 \pm 2.4$. The differences are not significant at the 95% confidence level, and so the 0.3-torr data are used in the analysis leading to the results in Table II.

TABLE III. Comparison of ionization cross sections of electrons and positrons on argon. The indicated uncertainties of measurement are relative standard deviations based on counted numbers.

Energy (MeV)	(σ for e^+)/(σ for e^-)
0.67	0.9960 ± 0.0057
1.10	1.0075 ± 0.0059
average	1.0015 ± 0.0041

VI. DISCUSSION

Comparison with Theory

A definitive comparison of our result with theory is possible for He. As first pointed out by Platzman (cf. footnote 11 of Ref. 13) in context with the McClure experiment, almost every excitation to a discrete state of He under our experimental conditions is converted to an ionization by process (a) or (b) discussed at the end of Sec. I. In other words, the η_n values of Eq. (4) may be taken, to a good approximation, as unity for every excited state n, both continuum and discrete. This particular situation justifies comparison of our results with the accurate theoretical values

$$M^2 = 0.7525 \quad \text{and} \quad C = 8.068,$$

given by Inokuti, Kim, and Platzman.[21]

All our results for M^2 with the three additives, H_2, Ar, and CH_4 (shown in Table II) agree with theory within random-error uncertainty. As for C, our result with H_2 as additive agrees with theory when possible systematic errors are considered. The satisfactory agreement with theory gives us confidence in the general correctness of our experimental procedure. Our C value with Ar as additive, however, is somewhat smaller than theory, and that with CH_4 as additive is smaller than theory by an extent definitely exceeding experimental uncertainty. We interpret the above finding as indicating that some of the excited He atoms that are converted into ionization by H_2 are quenched by CH_4; in other words, CH_4 is a less efficient converter of excitation to ionization than H_2.

Unfortunately, similar comparison is difficult in other cases because no theoretical data of comparable reliability appear available and because the efficiency at which discrete excitations are converted to ionizations under our experimental conditions is poorly known. Upper limits to M^2 in several cases, however, are either reasonably well known from theory or deducible from photoabsorption data.[13] In other words, a value of M^2 determined by our measurements should not exceed

$$M_{\text{tot}}^2 = \sum_n M_n^2 , \tag{14}$$

where the summation includes all excited states, discrete and ionized, for the atom or molecule under consideration. By virtue of a sum rule, the value of M_{tot}^2 can be computed from the ground-state wave function.[14,21] Our values of M^2 in Table II are not greater than theoretical M_{tot}^2 values for Ne (~2.0),[22] Ar (~5.5),[22] Kr (~7.9),[22] Xe(~10.3),[23] and H_2(1.549).[24]

Comparison with McClure's Results

As Table IV shows, our results agree fairly well with the earlier measurements of McClure,[5]

TABLE IV. Comparison of our data with McClure's data.

Atom or molecule	M^2 Present[a] Value	s.d.[c]	M^2 McClure[b] Value	s.d.[c]	C Present[a] Value	s.d.[c]	C McClure[b] Value	s.d.[c]
He	0.745	0.025	0.86	0.03	8.005	0.032	7.87	0.09
Ne	2.02	0.05	2.21	0.02	18.17	0.06	19.16	0.06
Ar	4.22	0.15	4.72	0.12	37.93	0.19	43.23	0.12
H_2	0.695	0.015	0.706	0.017	8.115	0.021	8.64	0.07

[a]For He, values with H_2 as additive are taken from Table II. For Ne and Ar, values with the *A* rating in Table II are used.

[b]Values have been derived from a reanalysis of the data of Table I, Ref. 5.

[c]Standard deviation estimated from least-squares analysis.

except for Ar. The reason for sizable discrepancies in the case of Ar remains obscure. We may only note that in an attempt to resolve these discrepancies, we have repeated numerous measurements and that our results have been quite reproducible.

Systematics of Our Data

For a comprehensive representation and in search for systematics, we have plotted all our data in Figs. 5–7.

In Figs. 5 and 6, where we plot M^2/N and C/N, respectively, as functions of the total number N of electrons in an atom or molecule, we find that at least two classes of systems are distinct; class I, including hydrocarbons and their derivatives shows higher values of M^2/N, roughly independent of N, while class II, including atoms and such molecules as CF_4 and BF_3, shows lower values of M^2/N that tend to decline with N. Although a full explanation of every data point will require detailed analysis, the general trend may be understood in part in the following way. The class-I systems have extended geometrical structure, and contain a substantial, and roughly constant, fraction of electrons in the valence shell. The class-II systems, in comparison, have tighter geometrical structure and contain a somewhat greater fraction of electrons in shells with higher binding energies; this situation is especially true for heavier atoms such as Xe and Hg, in which an appreciable number of electrons are subject to strong nuclear attraction. Notice that the quantity N/M^2 is an index of average energy transfer (measured in units of the Rydberg energy) for ionization by glancing collisions. [See Eq. (9) of Ref. 25.] The average energy transfer is smaller for class I than it is for class II.

Also, we observe a general similarity between Figs. 5 and 6. An implication of this similarity is that the ionization cross section, as given by Eq. (11), is nearly proportional to M^2, a fact that demonstrates the primary importance of the dipole contributions due to glancing collisions at high incident electron energies.[12,13]

The quantity C/M^2, whose reciprocal is plotted in Fig. 7, is an index of the effectiveness of hard collisions per atomic or molecular electron. That quantity should not be strongly dependent upon the system, and this is indicated by our data—especially when one considers that the possible systematic plus random error limits are rather large in comparison with the 30% range in the measured values. One should realize that it is possible to use the present data to determine ionization cross sections for nonrelativistic electrons ($T < 10^4$ keV) by noting

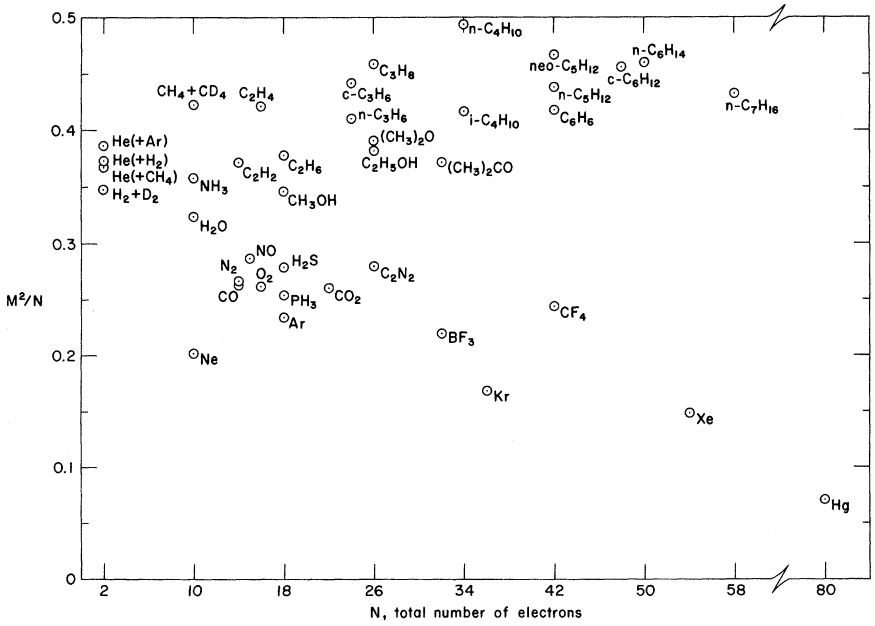

FIG. 5. Plot of M^2/N vs N, the total number of electrons in an atom or molecule.

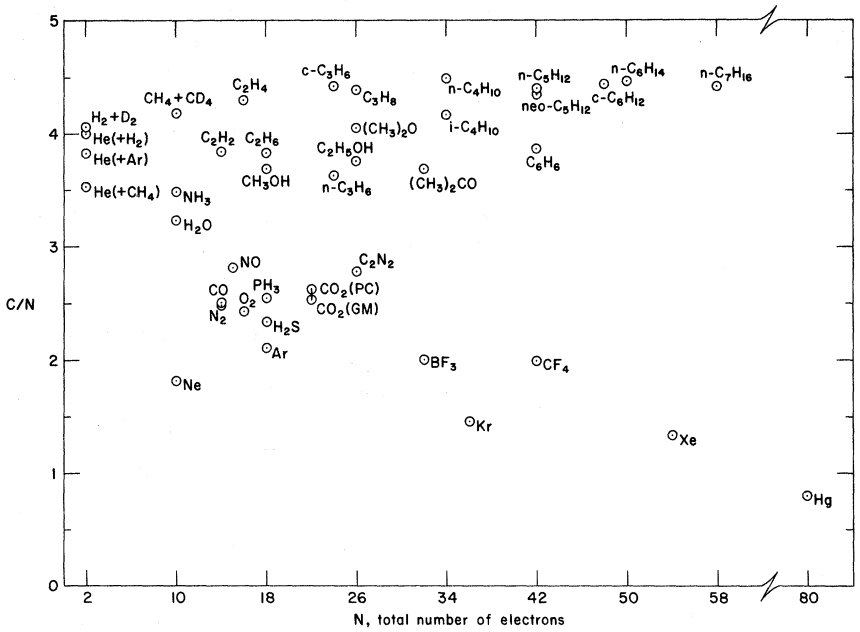

FIG. 6. Plot of C/N vs N, the total number of electrons in an atom or molecule.

that the Bethe cross section is then

$$\sigma = 4\pi a_0^2 (\mathcal{R}/T) M^2 \ln(4c_i T/\mathcal{R}) \ , \qquad (15)$$

where $T = \frac{1}{2}mv^2$, $v = \beta c$, a_0 is the Bohr radius, $\mathcal{R}$ the Rydberg energy, and c_i is related to C/M^2 by

$$\ln c_i = C/M^2 - 2\ln(2\hbar c/e^2) = C/M^2 - 11.2268 \ . \qquad (16)$$

(See Sec. 4.1 of Ref. 12.)

Additional comparisons with our data could be made for several gases with values of M^2 and C derived from other sources such as data taken at lower electron energies.[26] However, such comparisons must be made with care and these are reserved for a separate publication[27] that will also examine possible data systematics which have been explored in the past by Santar and Bednář.[28]

The present paper has presented the data and discussed the experimental technique for our determination of the cross section for ionization by fast electrons. Each gas presented individual

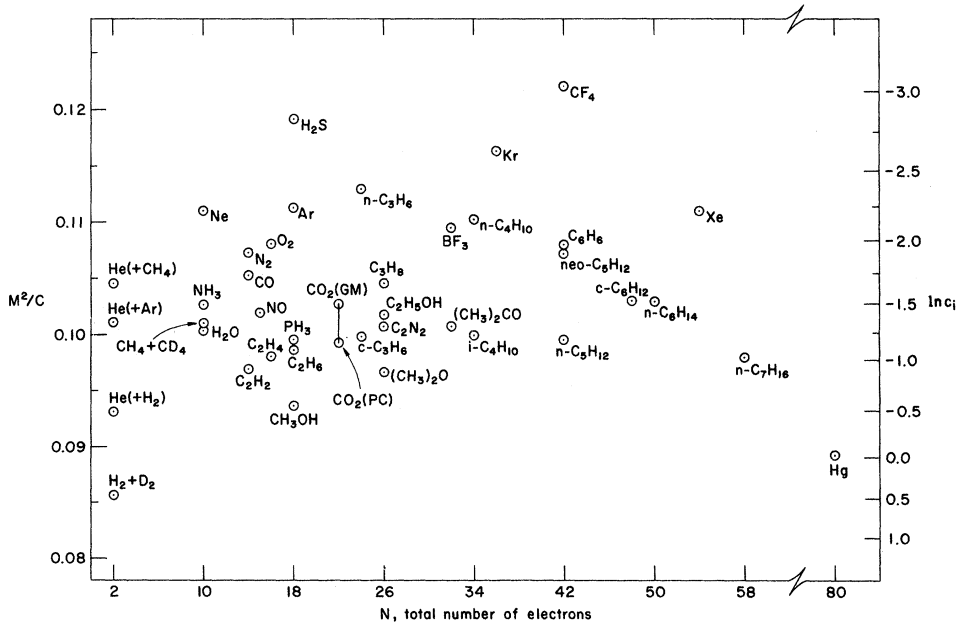

FIG. 7. Plot of M^2/C vs N, the total number of electrons in an atom or molecule. The nonlinear scale on the right-hand side is for $\ln c_i$ defined by Eq. (16), a quantity that characterizes the nonrelativistic Bethe cross section, Eq. (15).

problems in determining the proper operating conditions, and the data in Table II and Figs. 5–7 cover a wide variety of sample gases. It is hoped that these results will prove useful for workers in radiation physics and chemistry.

ACKNOWLEDGMENTS

The initial inspiration by Professor R. L. Platzman, as well as his continued encouragement, has been most valuable in the development of this research. Comments on the manuscript by Professor U. Fano and by some Argonne colleagues are also acknowledged.

APPENDIX

Many variations of quenching circuit have been tried; the one that has proved by far the most satisfactory is illustrated in Fig. 8, which also indicates the types of waveform that are involved. The resistance R_1, to some extent, acts as a normal quenching resistance; its effect is reinforced and sustained by the negative square wave applied through the direct-coupled vacuum tube V. The large disparity between the time constants $R_1(C_1+C_2)$ and R_4C_3 serves to attenuate the quench pulse at the input to the amplifier. In the amplifier, additional discrimination against slow-rising pulses helps to isolate the input of the quenching circuit from its output. In consequence, it is possible to adjust the circuit so that it will trigger on a 1-mV pulse at A, apply a −300-V quench pulse at D, and at the same time be stable against oscillation. Experience indicates that this high sensitivity is important even though the GM pulses normally saturate the amplifier. It appears that the circuit may lose control when a GM discharge occurs at the tail of the quench pulse, for then the voltage is only very slightly above threshold, as at d, and is too small to activate the quenching circuit.

In addition to B, the pulse generator supplies the two wave forms E and F. The square wave F is supplied to a coincidence circuit that registers coincidences between responses of the GM and silicon detectors; as normally adjusted it is eight microseconds long. The pulse G from the silicon detector is delayed four microseconds before entering the coincidence circuit. The square wave E is two hundred microseconds longer than B; it is supplied to an anticoincidence circuit to reject those pulses from the silicon detector that occur while the voltage on the GM counter is below its normal value; silicon pulses that fall within F are counted as coincidences (the $d\cdot g$ channel in Fig. 1); those outside of E are counted as anticoincidence (the $d\cdot\bar{g}_s$ channel); the remaining ones are not counted at all.

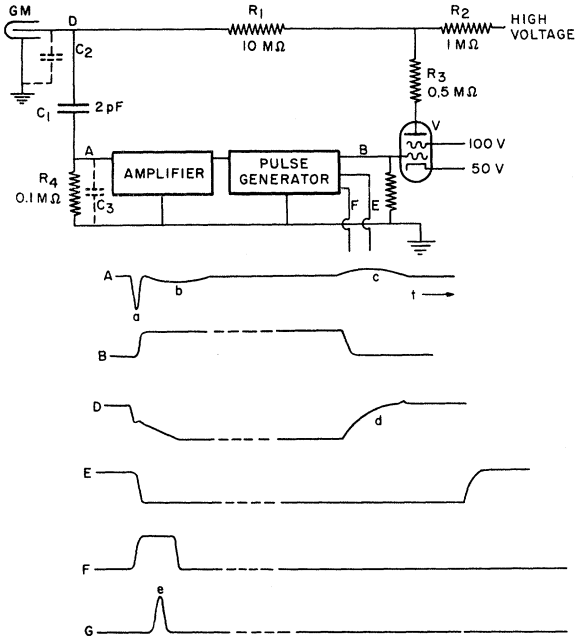

FIG. 8. The quenching circuit used for GM counting and waveforms in the circuit. (See Appendix.)

*Work performed under the auspices of the U. S. AEC.

†Deceased. The present manuscript has been prepared from Dr. Rieke's draft by M. Inokuti and J. C. Person of ANL to either of whom correspondence concerning this paper may be addressed.

[1]Much of the early work on this subject has been published under the title "Specific Primary Ionization" (SPI). The SPI, denoted by S, is defined as the number of primary ionization events per unit path length of primary particles through a gas at 0 °C and 760 torr; it is related to the cross section by $S=2687\sigma$, where S is in units of cm^{-1} and σ in 10^{-16} cm^2.

[2]C. T. R. Wilson, Proc. Roy. Soc. (London) A104, 192 (1923).

[3]E. J. Williams and F. R. Terroux, Proc. Roy. Soc. (London) A126, 289 (1930).

[4]T. Graf, J. Phys. Radium 10, 513 (1939).

[5]G. W. McClure, Phys. Rev. 90, 796 (1953).

[6]F. F. Rieke and W. Prepejchal, in (a) Argonne National Laboratory Radiological Physics Division Annual Report for 1964–1965, ANL-7060, p. 33, 1965 (unpublished); (b) *ibid.* for 1965–1966, ANL-7220, p. 19, 1966; (c) *ibid.* for 1966–1967, ANL-7360, p. 50, 1967; (d) *ibid.* for 1967–1968, ANL-7489, p. 99, 1968; (e) *ibid.* for 1968–1969, ANL-7615, p. 214, 1969; (f) *ibid.* for 1969–1970, ANL-7760, Part I, p. 87, 1970.

[7]F. F. Rieke and W. Prepejchal, in *Abstracts of Papers, Third International Congress of Radiation Research, Cortina d'Ampezzo, Italy*, 1966 (Tipografia Regionale, Rome, 1966), p. 187.

[8]F. F. Rieke and W. Prepejchal, Bull. Am. Phys. Soc. 13, 37 (1968).

[9]F. F. Rieke and W. Prepejchal, in *Sixth International Conference on the Physics of Electronic and Atomic Collisions, Cambridge, Massachusetts*, 1969 (MIT U. P., Cambridge, Mass., 1969), p. 623.
[10]H. Bethe, Ann. Physik 5, 325 (1930).
[11]H. Bethe, in *Handbuch der Physik*, edited by H. Geiger and K. Scheel (Springer, Berlin, 1933), Vol. 24/1, p. 273.
[12]M. Inokuti, Rev. Mod. Phys. 43, 297 (1971).
[13]U. Fano, Phys. Rev. 95, 1198 (1954).
[14]R. L. Platzman, J. Phys. Radium 21, 853 (1960).
[15]R. Gold and E. F. Bennett, Phys. Rev. 147, 201 (1966).
[16]K. D. Carlson, P. W. Gilles, and R. J. Thorn, J. Chem. Phys. 38, 2725 (1963).
[17]R. H. Busey and W. F. Giauque, J. Am. Chem. Soc. 75, 806 (1953).
[18]R. L. Platzman, Vortex 23, 372 (1962).
[19]R. L. Platzman, J. Chem. Phys. 38, 2775 (1963).
[20]W. P. Jesse, J. Chem. Phys. 38, 2774 (1963).
[21]M. Inokuti, Y.-K. Kim, and R. L. Platzman, Phys. Rev. 164, 55 (1967).
[22]R. J. Bell and A. Dalgarno, Proc. Phys. Soc. (London) 86, 375 (1965).
[23]R. J. Bell and A. Dalgarno, Proc. Phys. Soc. (London) 89, 55 (1966).
[24]The value is for the ground vibrational and rotational state and is derived from Table VI of L. Wolniewicz, J. Chem. Phys. 45, 515 (1966).
[25]R. L. Platzman, in *Radiation Research* 1966, *Proceedings of the Third International Congress of Radiation Research, Cortina d'Ampezzo, Italy*, 1966, edited by G. Silini (North-Holland, Amsterdam, 1967), p. 20.
[26]B. L. Schram, A. J. H. Boerboom, and J. Kistemaker, Physica 32, 185 (1966); B. L. Schram, *ibid.* 32, 197 (1966); B. L. Schram, M. J. van der Wiel, F. J. de Heer, and H. R. Moustafa, J. Chem. Phys. 44, 49 (1966); J. Schutten, F. J. de Heer, H. R. Moustafa, A. J. H. Boerboom, and J. Kistemaker, *ibid.* 44, 3924 (1966).
[27]M. Inokuti and J. C. Person (unpublished).
[28]I. Santar and J. Bednář, Collection Czech. Chem. Commun. 34, 1 (1969); 34, 311 (1969); I. Santar, in *Progress and Problems in Contemporary Radiation Chemistry*, Vol. 1, edited by J. Teplý (Czechoslovak Academy of Sciences, Prague, 1971), p. 51; in Third Tihany Symposium on Radiation Chemistry, Balatonfüred, Hungary, 1971, Preprint ÚJV 2611-Ch (unpublished).

PHYSICAL REVIEW A VOLUME 6, NUMBER 4 OCTOBER 1972

Extreme-Wing Line Broadening and Cs-Inert-Gas Potentials*

R. E. M. Hedges,† D. L. Drummond, and Alan Gallagher‡
Joint Institute for Laboratory Astrophysics, University of Colorado, Boulder, Colorado 80302
(Received 6 April 1972)

The emission profiles of the cesium resonance lines broadened by collisions with inert gases have been measured from about 50–1000 cm^{-1} from line center. The emission is observed from optically excited Cs in a cell whose temperature is varied from about 300 – 800 °K. By measuring the wing intensity relative to the entire line intensity from optically thin Cs, the profiles can be related to theoretical models without knowledge of the cesium density. The quasistatic theory of line broadening, extended to include the distribution of perturber positions about the Cs^*, is used to analyze the data. The observed temperature dependence of the emission profiles is associated with the temperature dependence of the perturber distribution in the Cs*–inert-gas adiabatic potential. The quasistatic spectrum depends on the difference between excited- and ground-state adiabatic potentials, so each potential is thereby separately determined from the data. The $X\Sigma$, $A\Pi$, and $B\Sigma$ potentials for the 3.5–5-Å region are given.

I. INTRODUCTION

This paper reports measurements and explanations of the far-wing intensities of Cs resonance lines broadened by collisions with inert gases.[1a] We have measured emission from optically excited Cs in a cell whose temperature was varied. The cell contains typically 300 Torr of inert gas. The Cs is optically thin so that the ratio of wing to total emission intensity is meaningful without knowledge of the Cs density. This wing radiation, which we observe for 1000 Å from line center, is essentially a continuum. We describe it here in terms of the molecular radiation of unstable Cs–inert-gas molecules. The population distribution in the free and bound molecular states has a pronounced effect on this extreme-wing intensity distribution and we utilize the temperature dependence as a powerful diagnostic tool. This interpretation of the temperature-dependent wing profiles extends the quasistatic model originally formulated by Holtsmark, and developed by Kuhn, Jablonski, Margenau, Foley, Holstein, and others.[1–3] It allows the experimental data to be understood and unfolded to give the $Cs^*(6\,^2P)$ and $Cs(6\,^2S)$ adiabatic potentials for interaction with the inert gases in